University at Albany, State University of New York
Scholars Archive

Nanoscale Science & Engineering Honors College

5-2015

Alloy Solute Interactions at Grain Boundaries and Nanoscale Interfaces in Copper

Luke Prestowitz
University at Albany, State University of New York

Follow this and additional works at: https://scholarsarchive.library.albany.edu/honorscollege_nano

Part of the Nanoscience and Nanotechnology Commons

Recommended Citation
Prestowitz, Luke, "Alloy Solute Interactions at Grain Boundaries and Nanoscale Interfaces in Copper" (2015). *Nanoscale Science & Engineering*. 8.
https://scholarsarchive.library.albany.edu/honorscollege_nano/8

This Honors Thesis is brought to you for free and open access by the Honors College at Scholars Archive. It has been accepted for inclusion in Nanoscale Science & Engineering by an authorized administrator of Scholars Archive. For more information, please contact scholarsarchive@albany.edu.

Alloy Solute Interactions at Grain Boundaries and Nanoscale Interfaces in Copper

An honors thesis presented to the
Department of Nanoscale Engineering,
University at Albany, State University Of New York
in partial fulfillment of the requirements
for graduation with Honors in Nanoscale Engineering
and
graduation from The Honors College.

Luke Prestowitz

Research Mentor: Brendan O'Brien

Research Professor: Kathleen Dunn Ph.D.

May 2015

Abstract

To study grain boundary solute interactions we have developed recipes for co-electrodeposition of dilute copper alloys including Cu(Ni) and Cu(Co). Secondary Ion Mass Spectrometry (SIMS) was used to analyze the incorporation of solute into the copper film. In addition to the co-electrodeposition process we also used a drive-in diffusion model for Au, Ag, Co, and Ni. Atomic imaging in a scanning transmission electron microscope (STEM) was used to visualize and investigate solute at grain boundaries and interfaces in polygranular copper films. By understanding these interactions and pathways of alloying solutes in copper microstructures, we can more accurately predict alloying behavior and how they inhibit or promote grain boundary diffusion. Understanding how these alloys interact with grain boundary diffusion pathways and interfaces will, in turn, enable grain boundary and interface engineering solutions to obstacles faced by semiconductor manufacturers as more aggressive feature sizes are pursued.

Acknowledgements

I would like to thank Brendan O'Brien for all his patience, guidance, and help. Without him I would not have been able to get much of the information in this document. He did all of the TEM and Dual Beam work.

I would like to thank Kevin Musick, who took the time to train me on the FIB, and was always willing to help when I asked.

I would like to sincerely thank Dr. Kathleen Dunn, whose support and willingness to help me made this project possible. Her guidance was imperative to my success as a student, and she was always willing to take time to explain concepts to me. I will always be grateful for the chance she gave me.

Table of Contents

Introduction ______ page 4

Experimental Details ______ Page 6

Results ______ Page 8

Discussion ______ Page 9

Conclusions ______ Page 12

References ______ Page 13

Appendix ______ Page 14

Alloy Solute Interactions at Grain Boundaries and Nanoscale Interfaces in Copper

Luke C. Prestowitz, Brendan O'Brien, Dr. Kathleen Dunn

College of Nanoscale Science and Engineering, SUNY Poly. 257 Fuller Road Albany, NY 12203

Abstract: To study grain boundary solute interactions we have developed recipes for co-electrodeposition of dilute copper alloys including Cu(Ni) and Cu(Co). Secondary Ion Mass Spectrometry (SIMS) was used to analyze the incorporation of solute into the copper film. In addition to the co-electrodeposition process we also used a drive-in diffusion model for Au, Ag, Co, and Ni. Atomic imaging in a scanning transmission electron microscope (STEM) was used to visualize and investigate solute at grain boundaries and interfaces in polygranular copper films. By understanding these interactions and pathways of alloying solutes in copper microstructures, we can more accurately predict alloying behavior and how they inhibit or promote grain boundary diffusion. Understanding how these alloys interact with grain boundary diffusion pathways and interfaces will, in turn, enable grain boundary and interface engineering solutions to obstacles faced by semiconductor manufacturers as more aggressive feature sizes are pursued.

Keywords: Copper alloys, Grain boundary segregation, polygranular

1. Introduction

The semiconductor industry's adherence to Moore's Law is driving the scaling of integrated circuits to an ever-decreasing node size and thus line (wire) width every eighteen to twenty-four months. This drive to scale down interconnects in the back end of the line (BEOL) has led to increased difficulty in obtaining the desired properties, particularly low resistivity and large bamboo grain structures, and has decreased the reliability of integrated circuits [1], [2]. The following set of pictures in Figure 1, represents the expected grain growth process for copper blanket films. The initial as plated microstructure in (A), is very small and polygranular. Once the sample sits at room temperature for one to two hours (B), it then starts to exhibit large grains that grow rapidly from the original microstructure. After the rapid growth, they slow down, and the rest of the microstructure starts to grow at a more even pace. The resulting microstructure is polygranular with several large grains randomly distributed (C) [1].

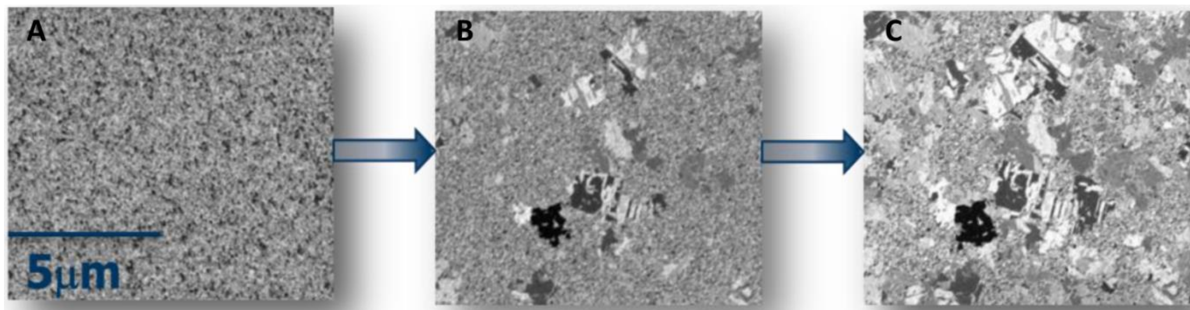

Figure 1: A) polygranular electrodeposited blanket copper film. B) Initial rapid grain growth. C) final microstructure

This microstructure in copper introduces significantly more parallel diffusion pathways for copper atoms, which at low temperatures dominates the movement of copper atoms, Figure 2(A). At the base of a via, where diffusion barrier material remains, the flux of copper ions from the upper wire is halted, while copper ions below the diffusion barrier continues to be swept down stream Figure 2(B). This flux imbalance [3] results in the formation of voids and causes the BEOL interconnects to fail much more quickly, Figure 2(C).

Previous work had shown that surface

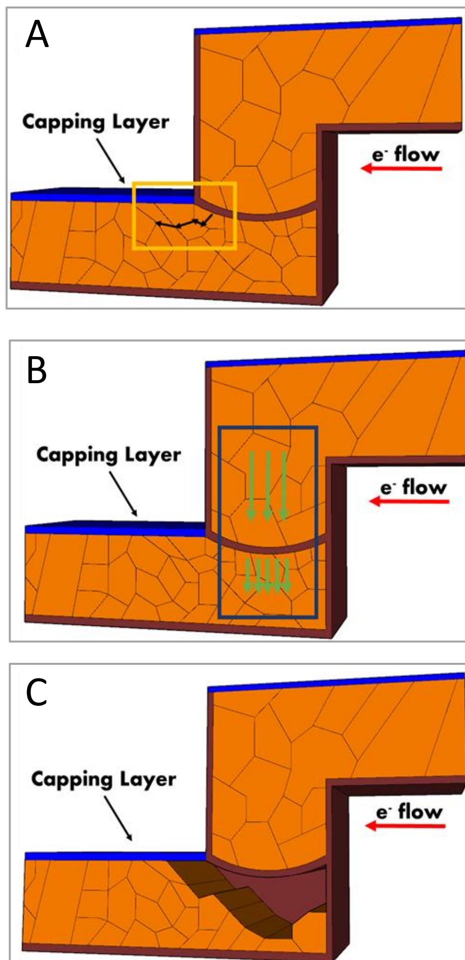

Figure 2: Electromigration failure process

diffusion mechanisms could be slowed or even eliminated to improve interconnect reliability, by using a capping layer such as cobalt tungsten phosphorus (CoWP) and cobalt. Although the capping layer can greatly increase the mean time to failure for copper interconnects up to 30x, the effect is muted (down to a 14x improvement) when the wires are polygranular [2]. Therefore, as lines get smaller, the grain boundaries will have a greater impact than the surface diffusion on the lifetime of the chip. Thus, since capping layers do not address the grain boundary (GB) diffusion, there needs to be alternative methods to controlling or hindering grain boundary diffusion. Prior to the use of copper in the BEOL interconnects, aluminum was the dominant metal of choice for the semiconductor industry, and like copper aluminum faced electromigration failures as a major reliability issue. Previous work on Aluminum interconnects has shown an increased lifetime by using an Al(Cu) alloy which generates precipitates at the GB, increasing the activation energy for diffusion, and thus prolonging the lifetime of the chip [3]. As a result of this work, aluminum, cobalt and manganese have been studied to see if they can slow down grain boundary diffusion in copper interconnects by segregating to the grain boundaries, in hopes that they increase the activation energy. However, these systems are not well understood and there are many conflicting reports as to their efficacy. One difficulty in improving interconnect performance through alloying is a lack of information regarding segregation interactions at grain boundaries and interfaces when minute concentrations are introduced into the copper lattice. Historically, solute was expected to pin grain boundaries, increase resistivity, and reduce diffusivity by grain boundary “stuffing”. More recent studies on grain boundary complexions suggest a more complicated relationship, which can explain these results

as well as cases where segregation increases mobility or enhances diffusion [4]. In order to better understand Cu alloy systems, we developed experiments to observe realistic conditions, in order to create the opportunity to understand the solute-grain boundary interactions, and from this develop working models to allow for engineering solutions to grain boundary diffusion failure mechanisms in copper interconnects.

2. Experimental Details

2.1 Sample Preparation

All samples were prepared using a circular rotating disk electrode (RDE) mount that was custom machined to fit a one inch square wafer piece. The wafer was taped to the holder using conductive copper tape to complete the circuit to allow for the electrodeposition of metals from solution. The sample was then covered with an acid resistant tape, and a small 0.2827 cm^2 circular opening was punched into the tape to allow the film to be deposited. Once the sample was finished it was immediately rinsed in deionized water and dried using nitrogen.

2.2 Capping Metal Solutions

For the Copper drive in diffusion samples, an Enthone™ copper electroplating solution was used to deposit a 600 nm film on a blanket silicon wafer with 50 nm of iPVD copper seed. The 600 nm thickness was chosen based on previous work that indicated films less than 500 nm may not recrystallize at room temperature, a process which is crucial for achieving large grained copper films [5], [6]. After the film was electroplated, the sample was immediately submerged into an electrodeposition solution containing the drive in metal of interest to reduce the possibility of a surface oxide forming that would prevent or inhibit diffusion. Table 1 shows the plating solution makeups for cobalt, nickel, and silver electroplating solutions. The silver electroplating process was different from the other metal solutions, in that to get sufficient thickness of silver without a powdery coating, a sulfuric acid solution was made without silver nitrate. In a separate beaker a molar of silver nitrate solution was made and added to the sulfuric acid at the same time as the electrode was submerged. The gold electroplating solution came from Craswell™ 24CT Gold plating solution. All samples were plated using a Biologic-SP50 power source and a RDE at 400 rpm. Table 1 indicates the deposition potential and time for each drive in sample.

2.3 Co-Electroplating Solutions

For the Cu(Ni) and Cu(Co) co-electrodeposition baths previous work in literature was used for the basis of the solutions [7], [8]. Table 1 shows the solution makeup for the codeposition baths and the plating potential and time for each co-electrodeposition sample. Each was plated using the RDE at 400 rpm and the electroplating program was set to plate a 600 nm thick film.

2.4 Sample Anneal

Each drive-in diffusion sample was made in duplicate so that one could be annealed at 250°C for 2 hours and the other at 400°C for 2 hours. The choice for 400°C anneal as the maximum temperature was to simulate that of the dielectric deposition in semiconductor manufacturing. This process is one of the highest temperatures that a wafer is exposed to during the manufacturing

Metal Capping Layer Solutions			
Metal Solution	Component 1	Component 2	Component 3
Cobalt	0.4 M $CoSO_4$	0.01 $CoCl_2$	0.5 M H_3BO_3
Nickel	0.1 M NiSO4	0.5 M H3BO3	-
Silver	1 M H_2SO_4	0.1 M $AgNO_3$	-

Co-electrodeposition solutions					
Metal Solution	Component 1	Component 2	Component 3	Component 4	Component 5
Cobalt	0.5 M $CoSO_4$	0.05 M $CuSO_4$	0.1 M H_3BO_3	0.5 M $Na_3C_6H_5O_7$	0.1 M H_2SO_4
Nickel	0.24 M NiSO4	0.05 M $CuSO_4$	0.1 M H_3BO_3	0.1 M H_2SO_4	-

Electroplating Programs for Capping Layer					
Metal	Potential (mV)	mA/cm^2	Time (s)	RPM (RDE)	Hot Entry
Co	(-) 800	-	20	400	yes
Ni	(-) 800	-	20	400	yes
Au	-	0.08	20	400	yes
Ag	-	5	20	400	yes

Co-electrodeposition Electroplating Programs					
Metal	Potential (mV)	mA/cm^2	Time (s)	RPM (RDE)	Hot Entry
Co	(-) 800	-	90	400	yes
Ni	(-) 800	-	90	400	yes

Table 1: Electroplating solution makeup and electroplating programs for drive in samples and co-electrodeposition samples.

process due to the risk of damaging the front end of the line (FEOL). Therefore, using temperatures exceeding 400°C would not be representative of real-world production use and would make any findings less attractive to implementing into current industrial processes.

The co-deposition samples were annealed at the same temperatures and times as the drive-in diffusion samples. When no recrystallization was observed, the annealing was increased to 500°C for 5 hours for the sake of understanding the process, even though it would not be a realistic thermal budget in a production facility.

2.5 TEM Sample Prep

In order to view the samples in the Titan aberration corrected scanning transmission electron microscopy (STEM), each sample was milled using a Focused Ion beam, in a dual beam SEM. Platinum was used to protect the surface of the TEM sample, and each sample was mounted onto the TEM grid using an Omniprobe.

2.6 Solute Concentration

Secondary Ion Mass Spectrometry (SIMS) was used to determine if the alloy metal was incorporated into the films and what the concentration profile was throughout the thickness of the film. The SIMS standards were made at the ion accelerator in the SUNY Albany physics

department, with a known dose for all alloying metals.

3. Results

3.1 SIMS

The SIMS plot in Figure 3 is representative for both the nickel and cobalt copper codeposition.

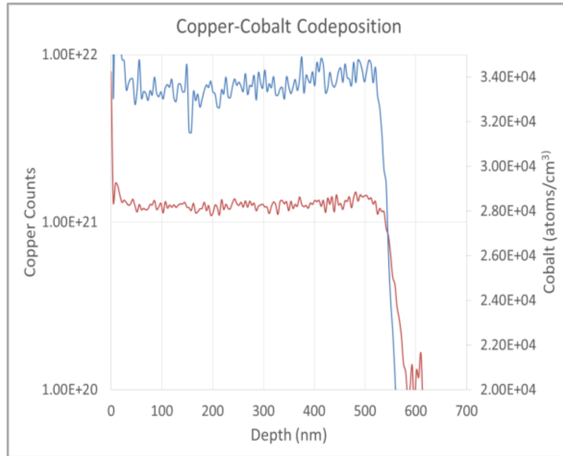

Figure 3: Sims profile of Copper-Cobalt Codeposition alloy, blue represents copper counts, the red cobalt.

It shows an even distribution of cobalt throughout the entire thickness of the copper film, the concentration of cobalt was on the order of 1.5 at%. In support of the SIMS data, the energy dispersive x-ray spectroscopy (EDX) map of the copper-cobalt alloy shows even cobalt distribution throughout the copper film in Figure 4. The nickel

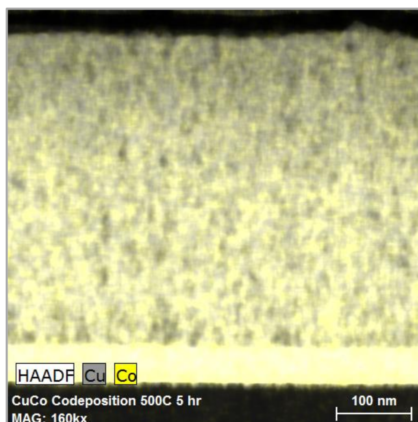

Figure 4: EDX map of Cu(Co) alloy annealed for 5 hours at 500 C^o.

codeposition sample likewise showed a similar SIMS profile indicating both baths performed as anticipated.

3.2 STEM and EDX Maps

Grain growth was anticipated in the copper-cobalt codeposition sample, however, as seen in Figure 5A the sample contains a multitude of small grains. After an initial 250°C/ 5 hour anneal, we did not observe any grain growth. Thus, we tried a second sample at 500°C for five hours Figure 5B. Again there is still very little grain growth present in the sample. In order to determine if the absence of grain growth was due to the cobalt pinning the grain boundaries or some additive in the bath, we made a plating solution with the same chemical make up as the copper-cobalt solution without the cobalt sulfate present. After electroplating this sample, we would expect to see grain growth for a 600 nm copper film at room temperature [5], [6]. However, the STEM image in Figure 5C clearly shows no grain growth occurred at room temperature. In all images, it can be seen that the seed layer, Figure 5D, is still

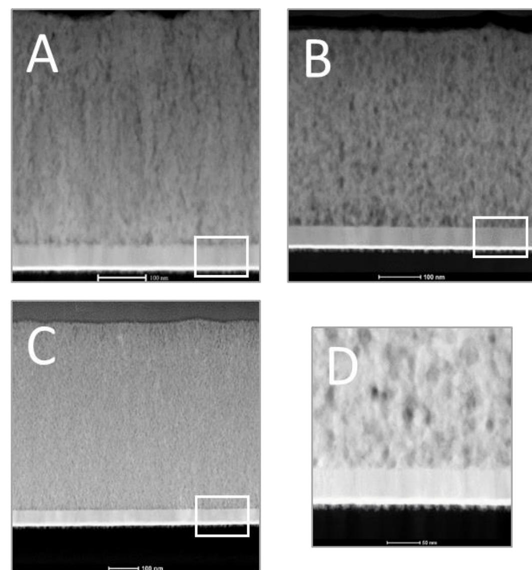

Figure 5: A,B) STEM image of Cu(Co) C)Pure copper film D) seed layer and film contrast

distinct from the electroplated film. This was not expected.

The following EDX map from the STEM Figure 6, depicts a cobalt drive in diffusion sample, there is no observable diffusion of cobalt from the surface into the film along the grain boundaries.

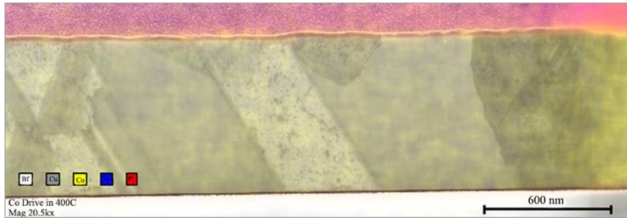

Figure 6: Co drive in diffusion at 400 Cº STEM EDX map

Also, there is no bulk diffusion of cobalt through the copper microstructure. Similarly to the cobalt drive in sample, the silver drive in diffusion sample as seen in Appendix Figure 1, did not show any observable diffusion of silver into the grain boundaries.

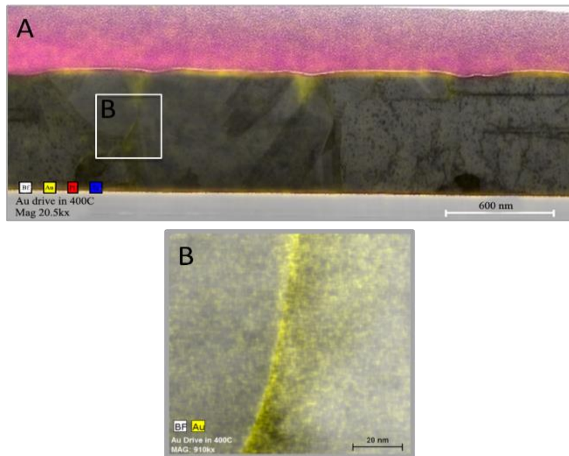

Figure 7: A) STEM EDX map of Au drive in diffusion sample at 400 Cº for 2 hours. B) The GB with Au segregation highlighted by the box in A.

For the gold drive in sample at 400°C anneal for 2 hours, significant grain boundary diffusion and segregation was detected by EDX in the STEM (Figure 7). It can be seen that the gold penetrates through the entire thickness of the blanket film.

For the nickel drive in diffusion at 400°C for 2 hours, we again observed grain boundary solute segregation in the copper film. The TEM sample in Figure 8 shows that the nickel diffused from the surface all the way to the silicon interface.

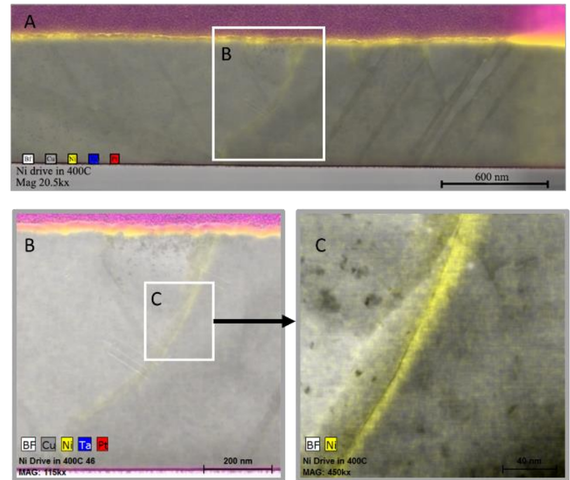

Figure 8: A) STEM EDX map of Ni drive in diffusion sample at 400 Cº for 2 hours. B) Magnified image of GB showing segregation. C) Magnified image of B

4. Discussion

The lack of grain growth in the cobalt system was not anticipated as the outcome for the codeposition films. In Zener pinning, impurities in the metal film apply a pinning pressure to the moving grain boundary which counter acts the driving force of grain boundary growth. If the pinning pressure cannot be overcome, the grains will not grow. The larger the impurity, the greater the pinning pressure it applies to the grain boundary. In order to determine if the pinning of the grain boundaries was due to the cobalt or the additives in the bath, we plated two samples. One sample was a pure copper bath using the same additives as the cobalt solution and the other solution included the cobalt. The aim was to see if the cobalt was pinning the grain boundary or if some other chemical agent was responsible. Due to

previous work, we know that pure copper films recrystallize at room temperature. It was expected that the pure copper film without the cobalt additive would recrystallize if the cobalt, which was not present, was responsible for the lack of recrystallization. Upon the analysis of this sample it was clearly seen that the pure copper did not show grain growth. Thus, we believe that the additives either the boric acid, trisodium citrate or a combination of the two was responsible for the Zener pinning.

One other unanticipated (and therefore interesting) observation from this experiment was the clear demarcation between the seed layer and the electrodeposited film. Normally the boundary between the iPVD seed layer and the electroplated copper is obliterated by the recrystallization process. In addition, because copper recrystallizes so quickly (within minutes, even at room temperature) it is not often that one is able to observe the true as-plated microstructure. As a result, being able to see the seed layer may lead to further studies to better understand what role it plays on the recrystallization of copper in interconnects and how this may impact the properties of the lines.

Since there was no grain growth in the cobalt codeposition sample, it is almost impossible to tell whether the cobalt was at the grain boundaries or evenly dispersed in the film. When looking at nanoscale interfaces in the STEM, even though it has picometer resolution laterally, you still need these interfaces to go through the entire thickness of the film since information is collected in projection. Since the signal is coming from transmitted electrons, if you have a 100 nm thick sample and each grain is 20 nm in diameter, you will be looking at 5 grains instead of one in that projection. As a result, the grain boundaries blur out and you cannot get atomic resolution of the solute at the grain boundary, instead you get an average of 5 different interfaces. This means that the fine grain structure will not allow you to see what is going on at the interface or grain boundary, nor will you be able to tell if you have solute segregation.

Thus in order to overcome this obstacle, drive in diffusion samples were made. Because we used the Enthone solution for the copper film, we did not have to worry about the additives from the codeposition bath preventing grain growth or recrystallization. In addition, by electroplating the alloy metal on top of the copper film, when annealing the sample, the copper grains will grow at the same time that the alloying metal diffuses into the grain boundaries. In all the drive in samples, the copper film recrystallized into a large grained microstructure allowing it to be more easily analyzed in the STEM.

Alloy	Celsius	D(cm^2/s)
Cu-Ni	400	9.00E-15
Cu-Au	383	4.00E-14
Cu-Ag	485	4.90E-14

Table 1: Cu alloy bulk diffusion coefficients near experimental operating temperatures.[11], [13]

As mentioned earlier in the results, the drive in samples for cobalt and silver did not exhibit grain boundary diffusion. The bulk diffusion coefficient for cobalt in copper at 400°C is approximately 10^{-17} cm^2/s [9], therefore, even if it was energetically favorable to reduce the excess free volume of the grain boundary by segregation of cobalt, it would not have been able to go very far. Longer anneal times may have allowed us to be able to observe grain boundary diffusion,

but on that time scale being able to implement the process into any high volume manufacturing process would be inefficient. In addition to cobalt's low diffusion coefficient, another factor for why there might not be large enough driving force for grain boundary segregation is that the phase diagram for a copper-cobalt alloy (Figure 9) shows a high immiscibility at low cobalt at%. Therefore, since cobalt does not like to be in contact with copper atoms, it would rather be on the surface with itself. In order for it to go into the grain boundary it would need to share two interfaces with copper, this increased surface area may require more energy than having an open volume at the interface.

The silver sample, which also did not

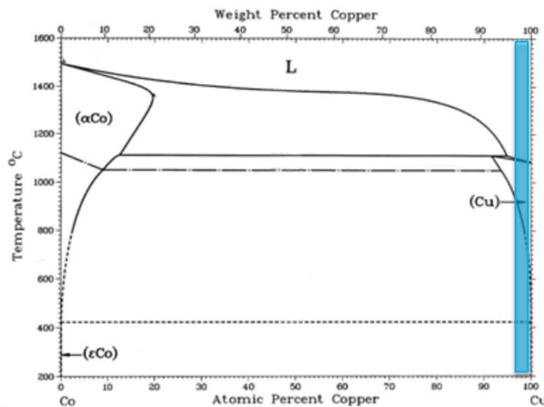

Figure 9: Copper Cobalt alloy phase diagram, the blue column represents the concentration of cobalt in copper and temperature range of the experiment. It shows very little solubility.

diffuse into the grain boundary, shares a similar phase diagram to that of cobalt. At high atomic percent copper-silver alloys, silver is not miscible in the microstructure. However, the diffusion coefficient for silver in copper is on the same order of magnitude as the gold and nickel Table 2.

Therefore, if one was to predict the segregation to grain boundaries on the diffusion coefficient, i.e. how easily it can get to the interface, one would expect to see segregation of silver. Since we did not observe segregation, it would indicate that the phase diagram more accurately dictates if segregation will occur, and that how easily a molecule will be able to diffuse through bulk copper microstructure is not a significant factor.

The nickel and gold drive in diffusion both showed significant segregation in the boundaries. In addition, both gold and nickel were able to diffuse through several hundred nanometers of the film thickness. Gold and nickel are completely miscible with copper when looking at their respective phase diagrams Figure 10 and Appendix Figure 2.

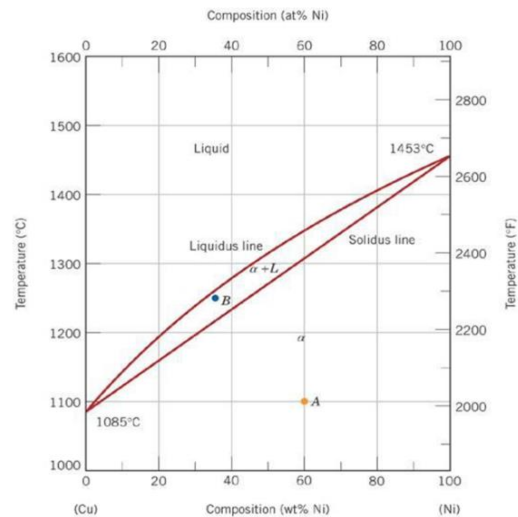

Figure 10: Copper-Nickel alloy phase diagram

In addition to the miscibility, both nickel and gold have similar diffusion coefficients in copper at 400°C Table 2. Both metals do not strongly differentiate between their own and copper atoms, in addition, they both have larger diffusion coefficients allowing for more rapid movement through the microstructure to grain boundaries. This combination contributes to the observed

segregation. Gold is not considered as a capping or alloying metal in copper/silicon integrated circuits due to its diffusion into silicon and the subsequent failure of the chip. However, the III-V nitrides do use Gold as a capping metal, therefore, understanding gold diffusion into copper may be beneficial to these systems.

5. Conclusions and Future Work:

The phase diagram of the alloy system strongly indicates if the solute metal will diffuse into the grain boundaries in copper. The driving force at 500°C for the reduction of excess free volume in high angle grain boundaries is less than the increased energy for the creation of two new surfaces in the cobalt and silver alloys. As a result of this observation, the semiconductor industry and academia have hoped that alloy seeds may diffuse into the grain boundaries of copper, this includes cobalt and manganese. Due to the study we know it is unlikely that cobalt will diffuse into the boundary, however, the phase diagram of manganese Appendix Figure 3 indicates it may be likely to diffuse into the grain boundary.

An additional property of elements that one cannot use to accurately predict the segregation properties of a solute, is the atomic radii of the atom. Although gold is has a larger radii than cobalt, the additional stress it may introduce into the lattice is insignificant, and it was able to segregate to the grain boundary. Therefore, one cannot predict segregation based on the similarity or dissimilarity in size of the elements in the alloy.

Previous work on a copper silver system at higher temperatures than used in this work [10] did show grain boundary segregation to high angle grain boundaries. Therefore, there may be an argument for the impact of the electronic structure of the metal on the segregation in copper. All three metals, silver, gold, and nickel have an S shell with 1electron, this is similar to the copper electronic structure as seen in table 3.

In conclusion, metals with a high solubility in copper have a higher probability of segregating to the grain boundaries, and similar electronic structures between the alloying metals may play an important role. In addition to these, a large difference in the diffusion coefficients of the solute in the bulk versus the grain boundary is an indicator that the alloy will successfully partition to the grain boundary interface. These diffusion coefficients for both metals that showed significant segregation can be seen in Table 4 [11]–[13].

Element	Electronic Structure
Au	[Xe] 4f14 5d10 6s1
Ag	[Kr] 4d^10 5s^1
Cu	[Kr] 4d^10 5s^1
Ni	[Ar] 3d9 4s1
Co	[Ar] 3d7 4s2

Table 2: Electronic structure of all elements used in diffusion

Solute	GB Diffusion	Lattice Diffusion
Ni	$D_{gb} \sim 10^{-7}$ cm^2/s	$D_{gb} \sim 7*10^{-3}$ cm^2/s
Au	$D_l \sim 10^{-16}$ cm^2/s	$D_l \sim 9*10^{-15}$ cm^2/s

Table 4: GB and Lattice diffusion coefficients for Au and Ni

More work needs to be done on studying the grain boundary solute interface to see what type of bonding or ordering is taking place. Understanding these bonding characteristics will be important in determining if the activation energy for grain boundary diffusion will be increased. For this to happen, we need to locate a high symmetry grain boundary in our sample that runs

through the entire thickness to get atomic level resolution. In combination with the images, we can also use Electron Energy Loss spectroscopy to observe the bonding characteristics of the solute copper interaction. Through these techniques we will then be able to predict with more accuracy the outcome of capping layers, alloy seeds, or codeposited films for copper interconnects.

References:

[1] M. Rizzolo, "The Influence of Impurities and Metallic Capping Layers on the Microstructure of Copper Interconnects," 2014.

[2] L. Zhang, J. P. Zhou, J. Im, and P. S. Ho, "Effects of Cap Layer and Grain Structure on Electromigration Reliability of Cu / Low-k Interconnects for 45 nm Technology Node," in *Reliability Physics Symmposium*, 2010, vol. 30, pp. 0–5.

[3] T. M. Shaw, C. Hu, K. Y. Lee, and R. Rosenberg, "The microstructural stability of Al (Cu) lines during electromigration," vol. 67, no. August 1995, pp. 2296–2299, 2001.

[4] P. R. Cantwell, M. Tang, S. J. Dillon, J. Luo, G. S. Rohrer, and M. P. Harmer, "Grain boundary complexions," *Acta Mater.*, vol. 62, no. 152, pp. 1–48, Jan. 2014.

[5] C. Detavernier, S. Rossnagel, C. Noyan, S. Guha, C. Cabral, and C. Lavoie, "Thermodynamics and kinetics of room-temperature microstructural evolution in copper films," *J. Appl. Phys.*, vol. 94, no. 5, p. 2874, 2003.

[6] S. Lagrange, S. . Brongersma, M. Judelewicz, a Saerens, I. Vervoort, E. Richard, R. Palmans, and K. Maex, "Self-annealing characterization of electroplated copper films," *Microelectron. Eng.*, vol. 50, no. 1–4, pp. 449–457, Jan. 2000.

[7] T. Cohen-Hyams, "Electrodeposition of Granular Cu-Co Alloys," *J. Electrochem. Soc.*, vol. 30, 2003.

[8] P. . Bradley and D. Landolt, "Pulse-plating of copper–cobalt alloys," *Electrochim. Acta*, vol. 45, no. 7, pp. 1077–1087, Dec. 1999.

[9] R. Döhl, "Measurement of the diffusion coefficeint of cobalt in copper," *Phys. status solidi. A. Appl. Res.*, vol. 86, no. 2, p. 603–, 1984.

[10] S. V. Divinski, H. Edelhoff, and S. Prokofjev, "Diffusion and segregation of silver in copper Σ 5(310) grain boundary," *Phys. Rev. B*, vol. 85, no. 14, p. 144104, Apr. 2012.

[11] M. Butrymowicz, Daniel Manning, John Read, "Diffusion in Cu Alloys - Part II. Copper-Silver and Copper-Gold Systems," *J. Phys. Chem. Ref. Data*, vol. 3, no. 2, 1974.

[12] C. Herzig and S. V. Divinski, "Grain Boundary Diffusion in Metals: Recent Developments," *Mater.*

Trans., vol. 44, no. 1, pp. 14–27, 2003.

[13] M. Butrymowicz, Daniel Manning, John Read, “Diffusion in Cu alloys - Part I. Volume and Self-Difussion in copper,” *J. Phys. Chem. Ref. Data*, vol. 2, no. 3, 1973.

Appendix

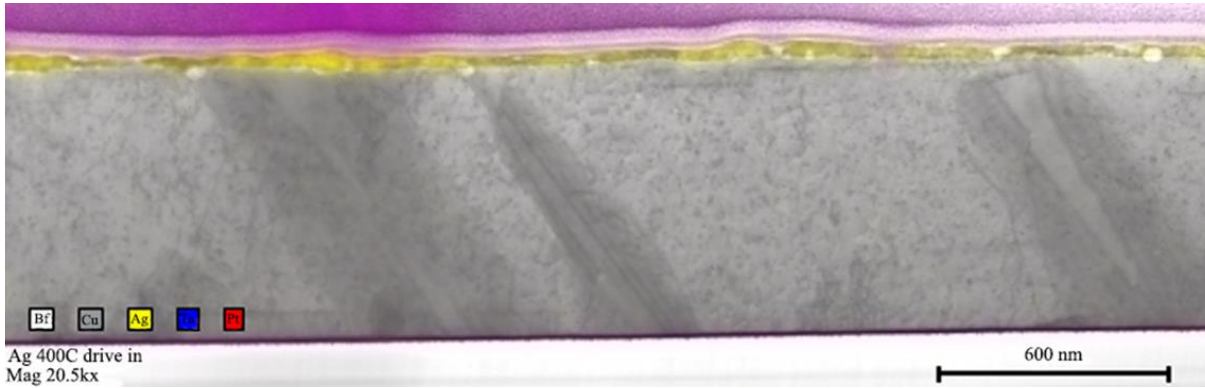

Figure 1: Silver drive in diffusion sample 400 C^o.

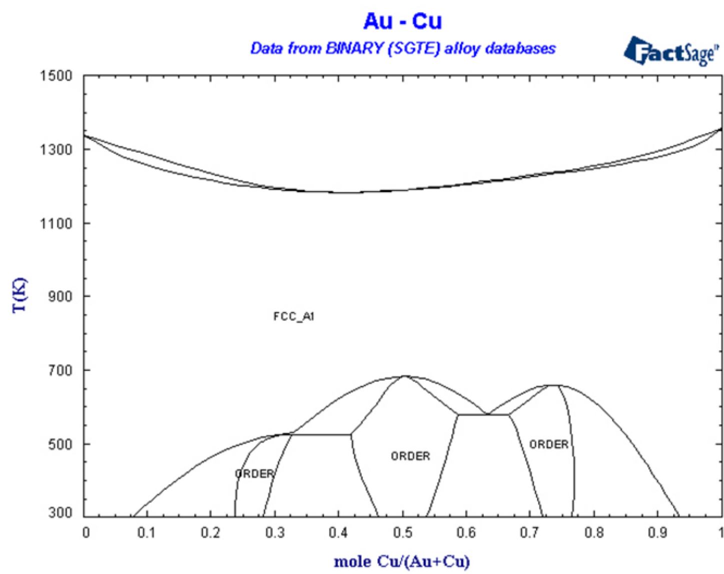

Figure 2: Gold-Copper alloy phase diagram

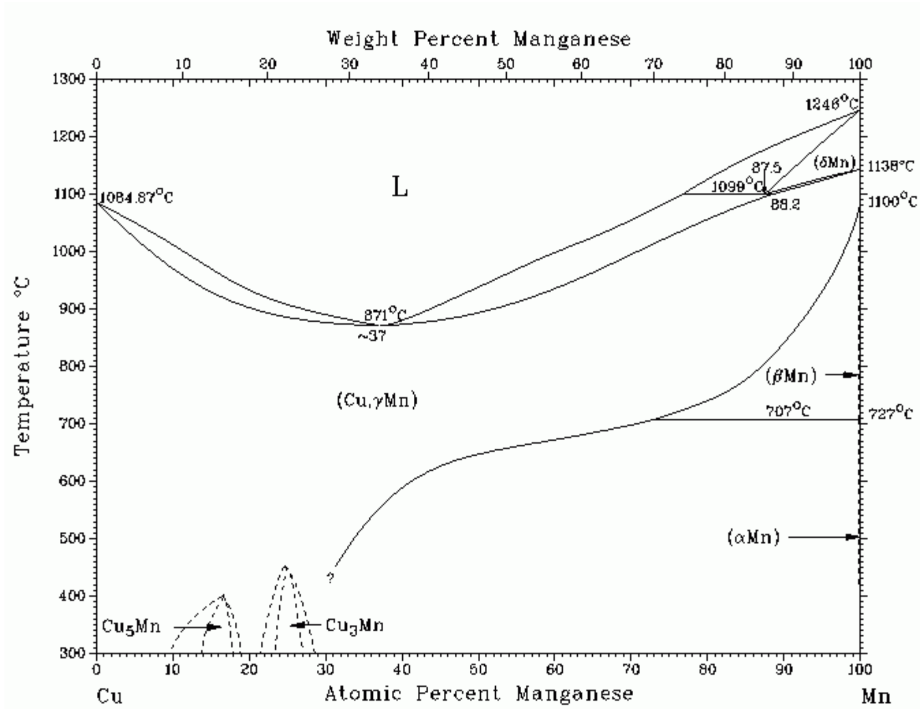

Figure 3: Copper-Manganese alloy phase diagram.